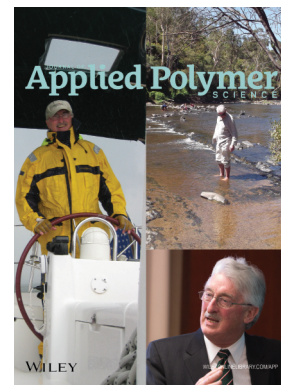


Special Issue: Sustainable Polymers and Polymer Science  
Dedicated to the Life and Work of Richard P. Wool

Guest Editors: Dr Joseph F. Stanzione III (Rowan University, U.S.A.)  
and Dr John J. La Scala (U.S. Army Research Laboratory, U.S.A.)



#### EDITORIAL

Sustainable Polymers and Polymer Science: Dedicated to the Life and Work of Richard P. Wool  
Joseph F. Stanzione III and John J. La Scala, *J. Appl. Polym. Sci.* 2016, DOI: [10.1002/app.44212](https://doi.org/10.1002/app.44212)

#### REVIEWS

Richard P. Wool's contributions to sustainable polymers from 2000 to 2015  
Alexander W. Bassett, John J. La Scala and Joseph F. Stanzione III, *J. Appl. Polym. Sci.* 2016,  
DOI: [10.1002/app.43801](https://doi.org/10.1002/app.43801)

Recent advances in bio-based epoxy resins and bio-based epoxy curing agents  
Elyse A. Baroncini, Santosh Kumar Yadav, Giuseppe R. Palmese and Joseph F. Stanzione III, *J. Appl. Polym. Sci.* 2016,  
DOI: [10.1002/app.44103](https://doi.org/10.1002/app.44103)

Recent advances in carbon fibers derived from bio-based precursors  
Amod A. Ogale, Meng Zhang and Jing Jin, *J. Appl. Polym. Sci.* 2016, DOI: [10.1002/app.43794](https://doi.org/10.1002/app.43794)

#### RESEARCH ARTICLES

Flexible polyurethane foams formulated with polyols derived from waste carbon dioxide  
Mica DeBolt, Alper Kiziltas, Deborah Mielewski, Simon Waddington and Michael J. Nagridge, *J. Appl. Polym. Sci.* 2016,  
DOI: [10.1002/app.44086](https://doi.org/10.1002/app.44086)

Sustainable polyacetals from erythritol and bioaromatics  
Mayra Rostagno, Erik J. Price, Alexander G. Pemba, Ion Ghiriviga, Khalil A. Abboud and Stephen A. Miller, *J. Appl. Polym. Sci.*  
2016, DOI: [10.1002/app.44089](https://doi.org/10.1002/app.44089)

Bio-based plasticizer and thermoset polyesters: A green polymer chemistry approach  
Mathew D. Rowe, Ersan Eyiler and Keisha B. Walters, *J. Appl. Polym. Sci.* 2016, DOI: [10.1002/app.43917](https://doi.org/10.1002/app.43917)

The effect of impurities in reactive diluents prepared from lignin model compounds on the properties of vinyl ester resins  
Alexander W. Bassett, Daniel P. Rogers, Joshua M. Sadler, John J. La Scala, Richard P. Wool and Joseph F. Stanzione III,  
*J. Appl. Polym. Sci.* 2016, DOI: [10.1002/app.43817](https://doi.org/10.1002/app.43817)

Mechanical behaviour of palm oil-based composite foam and its sandwich structure with flax/epoxy composite  
Siew Cheng Teo, Du Ngoc Uy Lan, Pei Leng Teh and Le Quan Ngoc Tran, *J. Appl. Polym. Sci.* 2016, DOI: [10.1002/app.43977](https://doi.org/10.1002/app.43977)

Mechanical properties of composites with chicken feather and glass fibers  
Mingjiang Zhan and Richard P. Wool, *J. Appl. Polym. Sci.* 2016, DOI: [10.1002/app.44013](https://doi.org/10.1002/app.44013)

Structure–property relationships of a bio-based reactive diluent in a bio-based epoxy resin  
Anthony Maiorana, Liang Yue, Ica Manas-Zloczower and Richard Gross, *J. Appl. Polym. Sci.* 2016, DOI: [10.1002/app.43635](https://doi.org/10.1002/app.43635)

Bio-based hydrophobic epoxy-amine networks derived from renewable terpenoids  
Michael D. Garrison and Benjamin G. Harvey, *J. Appl. Polym. Sci.* 2016, DOI: [10.1002/app.43621](https://doi.org/10.1002/app.43621)

Dynamic heterogeneity in epoxy networks for protection applications  
Kevin A. Masser, Daniel B. Knorr Jr., Jian H. Yu, Mark D. Hindenlang and Joseph L. Lenhart, *J. Appl. Polym. Sci.* 2016,  
DOI: [10.1002/app.43566](https://doi.org/10.1002/app.43566)

Special Issue: Sustainable Polymers and Polymer Science  
Dedicated to the Life and Work of Richard P. Wool

Guest Editors: Dr Joseph F. Stanzione III (Rowan University, U.S.A.)  
and Dr John J. La Scala (U.S. Army Research Laboratory, U.S.A.)

Statistical analysis of the effects of carbonization parameters on the structure of carbonized electrospun organosolv lignin fibers

Vida Poursorkhabi, Amar K. Mohanty and Manjusri Misra, *J. Appl. Polym. Sci.* 2016, DOI: 10.1002/app.44005

Effect of temperature and concentration of acetylated-lignin solutions on dry-spinning of carbon fiber precursors

Meng Zhang and Amod A. Ogale, *J. Appl. Polym. Sci.* 2016, DOI: 10.1002/app.43663

Poly(lactic acid) bioconjugated with glutathione: Thermosensitive self-healed networks

Dalila Djidi, Nathalie Mignard and Mohamed Taha, *J. Appl. Polym. Sci.* 2016, DOI: 10.1002/app.43436

Sustainable biobased blends from the reactive extrusion of polylactide and acrylonitrile butadiene styrene

Ryan Vadori, Manjusri Misra and Amar K. Mohanty, *J. Appl. Polym. Sci.* 2016, DOI: 10.1002/app.43771

Physical aging and mechanical performance of poly(L-lactide)/ZnO nanocomposites

Erlantz Lizundia, Leyre Pérez-Álvarez, Míriam Sáenz-Pérez, David Patrocínio, José Luis Vilas and Luis Manuel León, *J. Appl. Polym. Sci.* 2016, DOI: 10.1002/app.43619

High surface area carbon black (BP-2000) as a reinforcing agent for poly[(–)-lactide]

Paula A. Delgado, Jacob P. Brutman, Kristina Masica, Joseph Molde, Brandon Wood and Marc A. Hillmyer, *J. Appl. Polym. Sci.* 2016, DOI: 10.1002/app.43926

Encapsulation of hydrophobic or hydrophilic iron oxide nanoparticles into poly-(lactic acid) micro/nanoparticles via adaptable emulsion setup

Anna Song, Shaowen Ji, Joung Sook Hong, Yi Ji, Ankush A. Gokhale and Ilsoon Lee, *J. Appl. Polym. Sci.* 2016, DOI: 10.1002/app.43749

Biorenewable blends of polyamide-4,10 and polyamide-6,10

Christopher S. Moran, Agathe Barthelon, Andrew Pearsall, Vikas Mittal and John R. Dorgan, *J. Appl. Polym. Sci.* 2016, DOI: 10.1002/app.43626

Improvement of the mechanical behavior of bioplastic poly(lactic acid)/polyamide blends by reactive compatibilization

JeongIn Gug and Margaret J. Sobkowicz, *J. Appl. Polym. Sci.* 2016, DOI: 10.1002/app.43350

Effect of ultrafine talc on crystallization and end-use properties of poly(3-hydroxybutyrate-co-3-hydroxyhexanoate)

Jens Vandewijngaarden, Marius Murariu, Philippe Dubois, Robert Carleer, Jan Yperman, Jan D'Haen, Roos Peeters and Mieke Buntinx, *J. Appl. Polym. Sci.* 2016, DOI: 10.1002/app.43808

Microfibrillated cellulose reinforced non-edible starch-based thermoset biocomposites

Namrata V. Patil and Anil N. Netravali, *J. Appl. Polym. Sci.* 2016, DOI: 10.1002/app.43803

Semi-IPN of biopolyurethane, benzyl starch, and cellulose nanofibers: Structure, thermal and mechanical properties

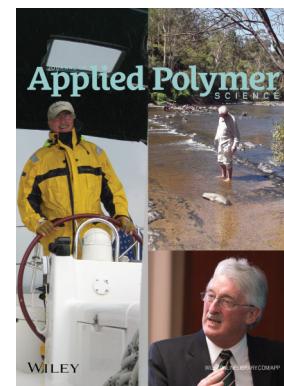
Md Minhaz-Ul Haque and Kristiina Oksman, *J. Appl. Polym. Sci.* 2016, DOI: 10.1002/app.43726

Lignin as a green primary antioxidant for polypropylene

Renan Gadioli, Walter Ruggeri Waldman and Marco Aurelio De Paoli *J. Appl. Polym. Sci.* 2016, DOI: 10.1002/app.43558

Evaluation of the emulsion copolymerization of vinyl pivalate and methacrylated methyl oleate

Alan Thyago Jensen, Ana Carolina Couto de Oliveira, Sílvia Belém Gonçalves, Rossano Gambetta and Fabricio Machado *J. Appl. Polym. Sci.* 2016, DOI: 10.1002/app.44129



## Mechanical behavior of palm oil-based composite foam and its sandwich structure with a flax-epoxy composite

Siew Cheng Teo,<sup>1,2</sup> Du Ngoc Uy Lan,<sup>1</sup> Pei Leng Teh,<sup>1</sup> Le Quan Ngoc Tran<sup>2</sup>

<sup>1</sup>School of Materials Engineering, Universiti Malaysia Perlis (UniMAP), Kompleks Taman Muhibah, Jejawi 2, 02600, Arau, Perlis, Malaysia

<sup>2</sup>Singapore Institute of Manufacturing Technology (SIMTech), A\*STAR, 71, Nanyang Drive, 638075, Singapore

Correspondence to: D. N. U. Lan (E-mail: uylan@unimap.edu.my)

**ABSTRACT:** Empty fruit bunch fiber (EFB), an abundant biomass waste from the palm oil industry, is used to reinforce palm oil-based polyurethane foam (POPU), and the mechanical properties of the composite foams are also assessed. The fiber–foam interfacial adhesion is also investigated by SEM images and Fourier transform infrared spectrometry. The results show that the composite foam reinforced by 15–30% EFB volume fractions could be enhanced by up to 10 times in flexural strength and twice in compressive strength compared to neat POPU. The composite foams with 20% and 30% volume fraction of EFB are exploited as a core in a sandwich construction with unidirectional flax fiber–reinforced epoxy composites (as face sheets). Sandwiches using EFB/POPU composite foam cores exhibited better toughness and achieved higher flexural energy at break compared to that using a commercial poly(ethylene terephthalate (PET) foam core. Furthermore, the failure mechanisms occurred under a combination of flexural and shear deformation. © 2016 Wiley Periodicals, Inc. *J. Appl. Polym. Sci.* **2016**, *133*, 43977.

**KEYWORDS:** fibers; foams; mechanical properties; polyurethanes; structure–property relations

Received 21 December 2015; accepted 23 May 2016

DOI: 10.1002/app.43977

### INTRODUCTION

Polyurethane foams have been widely used in sandwich structures thanks to their light weight and high mechanical properties. Commonly, rigid polyurethane foam is used as a core for sandwich materials, which is synthesized from petroleum-based polyol and methylene diphenyl diisocyanate (MDI). Regarding the constituents, MDI represents the least hazard and has a low vapor pressure that reduces its risks during handling compared to other major isocyanates, such as toluene diisocyanate (normally used in the synthesis of polyurethane foam).<sup>1</sup> Recently, because of the awareness of environmental preservation and sustainability, vegetable oil–derived polyols have been developed to replace or partially replace petroleum-based polyols, depending on the foam processing and final foam properties.<sup>2–5</sup> Vegetable oils, including soybean oil, canola oil, palm oil, and rapeseed oil, were converted to polyol through the introduction of hydroxyl functional groups into unsaturation sites and further to produce polyurethane foams.<sup>2,6,7</sup> Among the biopolyols, palm oil–based polyol is the most effective in producing the desired engineered polyurethane foam at low cost. In addition, the high homogeneity of palm oil–based polyol also provides a controllable foaming process, in which reinforcements (e.g., fibers) can be incorporated into the foam to enhance its properties.

Regarding fiber reinforcements, natural fibers such as flax, hemp, jute, kenaf, and palm oil fibers recently have received much interest thanks to their good mechanical properties and green characteristics. Among natural fibers, fibers extracted from the oil palm trunk, oil palm frond, palm pressed fiber, and the empty fruit bunch (EFB) are abundant and also have good properties.<sup>8,9</sup> The latter, EFB fiber, which is a bunch of fibers in which the palm fruits are embedded, consists of about 37.3–39.8% cellulose, 17.3–35.3% hemicelluloses, and 16.5–28.8% lignin.<sup>10,11</sup> These constituents are physically hard and strong. In addition, the lignin content in EFB has also been reported as being higher than that in banana, pineapple, and even soft and hardwood fiber.<sup>12</sup> It is also known that lignin contributes to the toughness of the fiber; therefore, EFB could be promising as a positive fiber for composites in terms of mechanical performance. When being used as a fiber for polyurethane composites, it is believed that the reaction between lignin, the hydroxyl group of the cellulose structure of EFB, and isocyanates forms a strong chemical bond between EFB fiber and the polyurethane matrix.<sup>13–16</sup> Researchers have also reported the use of palm oil biomass such as EFB and palm shells to reinforce the high-density rigid polyurethane core exhibiting high stiffness and the

flexural strength of a polyurethane-jute woven/vinyl ester composite sandwich.<sup>17</sup>

In sandwich constructions, the face sheets of the sandwich withstand the in-plane compressive and tensile stresses resulting from the flexural load, while the core, which is normally thick and much lower in density than the face sheets, resists and transmits shear force by keeping the two face sheets apart at the desired distance.<sup>18</sup> For face sheet materials, a long natural fiber composite can be a good candidate, such that some natural fiber composite systems (e.g., flax and hemp composites with epoxy) have mechanical properties comparable to glass fiber composites.<sup>19</sup> The combination of face sheets of long natural fiber composites and a biobased foam core may provide an ecofriendly sandwich construction with high mechanical performance.

In this study, composites of EFB fibers and biobased polyurethane foam are prepared and investigated. Various fiber volume fractions from 15 to 30% are incorporated into the foam. The properties of the composite foam, including morphology, fiber-foam interfacial adhesion, and mechanical properties, are then characterized. Then the foam is used as a core in a sandwich construction in which unidirectional flax fiber reinforced epoxy is implemented as the face sheets in the sandwich. Three-point bending tests are then performed on the sandwich samples to evaluate the mechanical properties of the materials. The sandwich fracture mode and the contribution of the core and the face sheets to the sandwich properties are presented and discussed accordingly.

## EXPERIMENTAL

### Materials and Preparation of EFB-Reinforced Foam

The palm oil-based polyol R3110 (equivalent weight 510 g/eq) was offered by PolyGreen Chemicals Sdn. Bhd. (Kuala Lumpur, Malaysia), and 4,4'-methylene bis(phenyl isocyanate) (MDI) with an equivalent weight of 125 g/eq was purchased from Maskimi Polyol Sdn. Bhd (Selangor, Malaysia). EFB fiber was obtained from DST Technology Sdn. Bhd (Penang, Malaysia) for use as reinforcement for the foam. The EFB fibers were washed and dried in an oven at 80 °C for 24 h and then put through a grinding process to produce short fibers. By using a centrifugal mill machine with mesh diameter 2.06 mm, fiber lengths in the range of 6–13 mm were obtained.

A biopolyurethane composite foam was prepared with the target density of 0.30 g cm<sup>-3</sup>. (Weight ratio 1:1) and distilled water of 5 parts per hundred resin (phr) were mixed at 400 rpm for 3 min using a stirrer. The resin mixture was modified based on an isocyanate index of 1.05. Equation (1) was used to calculate the total weight of MDI required.<sup>20</sup> The EFB fibers were mixed homogeneously (for 3 min) with the resin mixture, and the final compound was cast into a wooden mold (previously covered by polypropylene film to facilitate sample release). The mixture was cured for 24 h at room temperature. The EFB fiber concentrations were used at 15, 20, and 30 volume percentage (vol %) with respect to the mold cavity.

$$\text{wt.MDI} = (\text{index})(\text{MDI eq.wt.}) \left( \frac{\text{pbw of polyol A}}{\text{eq. wt. of polyol A}} + \frac{\text{pbw of H}_2\text{O}}{\text{eq. wt. of H}_2\text{O}} \right) \quad (1)$$

where wt, eq. wt, and pbw are weight, equivalent weight, and part by weight of resin, respectively.

### Materials and Processing of Flax-Epoxy Composite Face Sheets

A unidirectional (UD) flax-epoxy composite was used for the face sheets in the sandwich construction. Epolam 5015, a bisphenol-F-epichlorohydrinhydride epoxy resin and a curing agent consisting of 3-aminomethyl-3,5,5-trimethylcyclohexylamine and polyoxyalkyleneamine supplied by Axson Technologies (St. Ouen l'Aumon, France), was used as the composite matrix and adhesive between the face sheets and the foam core. The UD flax fibers with an areal density of 200 gm<sup>-2</sup> were provided by Lineo (Meulebeke, Belgium). The UD flax-epoxy composite face sheet was fabricated using the vacuum-assisted resin transfer method (VARI), and the composite was subjected to a post-curing process at 80 °C for 16 h. The composite face sheet was designed with a thickness of around 2 mm and fiber volume fraction of approximately 0.30.

### Preparation of Structural Sandwich

Sandwiches of the UD flax-epoxy composite face sheets and the composite foam core consisting of EFB and palm oil-based polyurethane (POPU) as well as the commercial poly(ethylene terephthalate) (PET) foam Airex T90 (3A Composites, Industrie Nord, Switzerland) were prepared by a bonding process using the Epolam epoxy resin system (which is the same as the matrix system of the flax-epoxy composite). The bonding was carried out at a low pressure of 0.1 MPa to avoid the foam being plastically compressed. The curing conditions for the epoxy were set at 120 °C for 20 min. Sandwich samples were cut in the dimensions of 200 mm × 40 mm × 2 mm for mechanical testing. A sandwich using commercial PET foam Airex T90 was used as a reference structural sandwich for comparison with the EFB/POPU sandwich. The commercial Airex T90 is one of the most common cores for sandwich applications because of its high compressive strength, which is the key point for the selection of a foam to be used as a sandwich core.<sup>21,22</sup>

### Investigation of EFB-Foam Interfacial Bonding, Foam Density, and Mechanical Properties of Composite Foams

To examine the possibility of EFB fiber and MDI reaction, dried EFB was impregnated with MDI and placed in a desiccator for 24 h (to avoid reaction of moisture and MDI). The interfacial bonding between EFB fiber and MDI was characterized using Fourier transform infrared spectroscopy (FTIR).

Bulk density ( $d_B$ ) is defined as the mass of a material divided by the total volume it occupies. Because the POPU obtained has an open-cell structure, the skeletal density ( $d_s$ ), the density of the solid polyurethane, was measured using a helium pycnometer apparatus. The porosity percentage,  $P$ , thus could be calculated using eq. (2)<sup>23</sup>:

$$P = \left( 1 - \frac{d_B}{d_s} \right) \times 100\% \quad (2)$$

A flatwise compressive test was conducted according to ASTM D1621 on the biobased composite foam specimens of

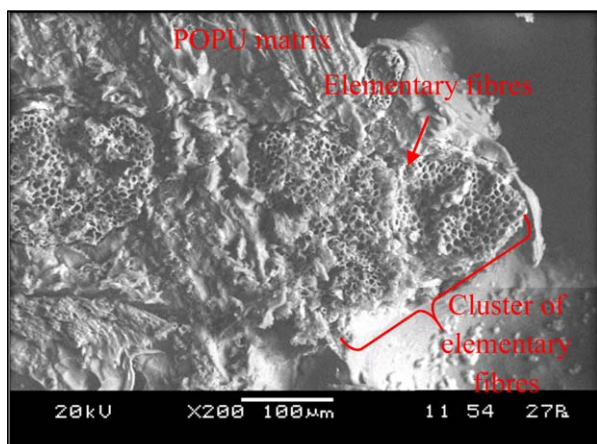


**Figure 1.** Cross section of EFB fiber reinforced POPU foam. [Color figure can be viewed in the online issue, which is available at [wileyonlinelibrary.com](http://wileyonlinelibrary.com).]

50 mm × 50 mm × 25 mm. The compressive test was carried out with a displacement rate of 5 mm/min and a 100 kN load cell.

The flexural property of the composite foam was investigated by three-point bending tests, which were performed in accordance with ASTM C393. Test specimens of the foam were prepared with dimensions of 200 mm × 50 mm × 25 mm. The test span length was set at a span-to-depth ratio of 6, and the testing speed was at 5 mm/min. The flexural toughness was derived from the area under the stress–strain curve of the composite foam. For both compressive and bending tests, at least five specimens were characterized.

#### Mechanical Testing of UD Flax–Epoxy Composite Face Sheets

The mechanical properties of the flax–epoxy composites were assessed by tensile and flexural tests. The tensile test was performed on the composites (specimen dimensions of 220 mm × 20 mm × 2 mm) with an Instron universal testing machine, (Massachusetts, United States) according to ASTM D3039. The testing speed was set at 5 mm/min, and a load cell of 100 kN was used. A three-point bending test on the composites was carried out in both the transverse and longitudinal directions according to ASTM D790. A testing speed of 5 mm/min was used, and the test span length was set at 48 mm. The fracture surface of the tested specimens was then investigated using a Zeiss EVO 50 XVP scanning electron microscope.

#### Evaluation of Mechanical Behavior of Sandwich Structure

The mechanical properties of the sandwiches were assessed by the three-point bending test according to ASTM C393. Sandwich specimens were prepared with dimensions of 200 mm × 50 mm × 25 mm. The support span-to-depth ratio was set to 6, and the testing speed was 5 mm/min. The contributed strength of the UD flax–epoxy face sheet and the biobased foam core with the sandwich panels under the three-point bending test can be estimated using the following equations. The maximum flexural stress  $\sigma_f$  carried by the bottom face sheet for a sandwich panel is calculated using eq. (3)<sup>24</sup>:

$$\text{Flexural strength carried by face sheet: } \sigma_f = \frac{PL(\frac{c}{2} + t)E_f}{4EI} \quad (3)$$

The limit load for face sheet yielding is calculated using eq. (4):

$$\text{Max. load for face yielding, } P_{lim} = \frac{4\sigma_f bt(c+t)}{L} \quad (4)$$

where  $L$  = Span length;  $b$  = width of core;  $E_c$  = Young's modulus of core.

The shear stress  $\tau_c$  experienced by the core for a sandwich panel is given by eq. (5)<sup>25</sup>:

$$\text{Core shear strength, } \tau_c = \frac{P}{2bc} \quad (5)$$

where  $t$  and  $c$  are the thickness of the face sheet and core, respectively, and  $P$  and  $E_f$  are the load applied and modulus of elasticity of the face sheet, respectively. The equivalent flexural stiffness ( $EI$ ) is as follows<sup>26,27</sup>:

$$\text{Flexural stiffness, } EI = \frac{E_f bt(c+t)^2}{2} + \frac{E_f bt^3}{6} + \frac{E_c bc^3}{12} \cong \frac{E_f btc^2}{2} \quad (6)$$

## RESULTS AND DISCUSSION

### Interfacial Bonding between EFB and POPU

Figure 1 shows an SEM image of a cross section of an EFB-reinforced biobased polyurethane foam, in which a good impregnation of the EFB into the POPU matrix can be observed. EFB fibers have a rough surface that may create a physical interlocking at the interface between the fiber and the matrix. Interfacial adhesion is likely from the strong covalent bonds between the hydroxyl groups on the fiber surface with the carbonyl groups of POPU. In addition, chemical interactions could occur between the hydroxyl groups of EFB and the isocyanate groups of MDI.

Figure 2 presents the FTIR spectrum of EFB fiber and MDI-impregnated EFB. The reaction of EFB and MDI occurs between the  $C_6-OH$  of the glucopyranose unit in the cellulose, the phenolic hydroxyl group in the lignin, and isocyanate to form urethane linkages.<sup>28–30</sup> The FTIR spectrum of MDI-impregnated

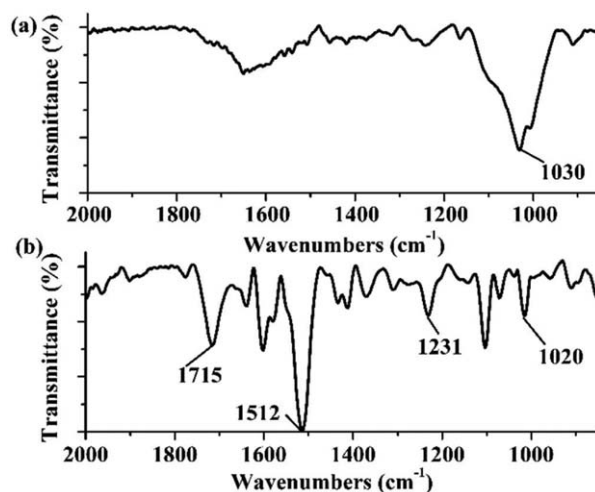


**Figure 2.** FTIR spectra of (a) EFB fiber and (b) MDI-impregnated EFB.

**Table I.** Flexural and Compressive Properties of Neat POPU and EFB/POPU Composite Foams

Physical properties	POPU	EFB15/POPU	EFB20/POPU	EFB30/POPU
Bulk density ( $\text{g cm}^{-3}$ )	0.13 ( $\pm 0.02$ )	0.29 ( $\pm 0.02$ )	0.29 ( $\pm 0.02$ )	0.29 ( $\pm 0.02$ )
Skeletal density ( $\text{g cm}^{-3}$ )	1.21 ( $\pm 0.03$ )	1.24 ( $\pm 0.06$ )	1.22 ( $\pm 0.02$ )	1.28 ( $\pm 0.01$ )
Total porosity percentage (%)	89.7 ( $\pm 0.90$ )	76.7 ( $\pm 1.80$ )	76.2 ( $\pm 1.70$ )	77.5 ( $\pm 1.70$ )
Mechanical properties	POPU	EFB15/POPU	EFB20/POPU	EFB30/POPU
Compressive modulus (MPa)	1.45 ( $\pm 0.04$ )	3.81 ( $\pm 0.13$ )	5.49 ( $\pm 0.03$ )	7.25 ( $\pm 0.01$ )
Compressive strength (MPa)	0.08 ( $\pm 0.07$ )	0.12 ( $\pm 0.03$ )	0.36 ( $\pm 0.09$ )	0.74 ( $\pm 0.07$ )
Densification strain (%)	74.1 ( $\pm 0.39$ )	73.4 ( $\pm 0.26$ )	69.5 ( $\pm 0.23$ )	68.6 ( $\pm 0.25$ )
Flexural modulus (MPa)	3.90 ( $\pm 0.26$ )	19.5 ( $\pm 1.18$ )	19.6 ( $\pm 1.45$ )	22.8 ( $\pm 1.62$ )
Flexural strength (MPa)	0.22 ( $\pm 0.01$ )	1.06 ( $\pm 0.03$ )	1.40 ( $\pm 0.06$ )	2.19 ( $\pm 0.09$ )
Flexural toughness (MPa)	0.03 ( $\pm 0.01$ )	0.08 ( $\pm 0.01$ )	0.17 ( $\pm 0.02$ )	0.39 ( $\pm 0.06$ )
Deflection at break (%)	17.3 ( $\pm 0.01$ )	13.3 ( $\pm 0.93$ )	14.6 ( $\pm 0.25$ )	19.9 ( $\pm 0.60$ )

EFB shows the new formation of carbonyl urethane ( $\text{—C=O}$  at  $1715 \text{ cm}^{-1}$ ), a secondary amide in urethane ( $\text{CN—H}$  at  $1512 \text{ cm}^{-1}$ ), and ether urethane ( $\text{—C—O—C}$  at  $1231 \text{ cm}^{-1}$ ), which present the urethane linkages.<sup>31–33</sup> Another supporting piece of evidence is the reduction of the peak at  $1020 \text{ cm}^{-1}$ , which represents the stretching vibration of aliphatic primary and secondary alcohols in cellulose, hemicellulose, lignin, and extractives.<sup>30,34,35</sup>

#### Effect of EFB on Density, Porosity, and Morphology of POPU Composite Foams

The bulk density, skeletal density, and porosity of neat POPU and EFB-reinforced POPU composite foams are reported in Table I. Bulk densities for the EFB/POPU composite foams of around  $0.3 \text{ g cm}^{-3}$  are achieved as targeted. The skeletal densities of the POPU control foam and the EFB/POPU composite foams are quite similar: approximately  $1.2 \text{ g cm}^{-3}$ . The addition of EFB produces a lower porosity in the EFB/POPU composite foams compared to neat POPU foam. This is because the pore volume of the composite foam was occupied by denser EFB fibers. In addition, the EFB fibers can affect the reactivity of the polyol and isocyanate and can interfere with foam expansion. A similar result was also reported in another study about rice husk ash-reinforced polyurethane.<sup>36</sup> The microscopy images of the cross sections of neat POPU foam and EFB/POPU composite foams are reported in Figure 3, which reveal that an increase in the EFB fiber content induces a corresponding decrease in porosity of the EFB/POPU composite foams. As observed, the length of the EFB fiber is much longer than the foam cell size. Therefore, most of the EFB fibers crossed many foam cells and are located parallel to the polyurethane's cell walls, a phenomenon that is expected to enhance the compressive strength of EFB/POPU composite foams. This phenomenon can also be found in the distribution of hemp fiber and flax fiber in a polyurethane matrix, which are also dispersed parallel to the cell walls of polyurethane.<sup>4</sup>

#### Effect of EFB Fibers on Mechanical Properties of EFB/POPU Composite Foam

**Compressive Properties of EFB/POPU Composite Foam.** As observed from the typical stress–strain curves of neat POPU foam and 30% EFB reinforced POPU foam (EFB30/POPU) (Figure 4), the compressive strength and densification strain are

derived. There is no yield deformation that occurred before 10% strain; therefore, the stress at 10% strain is selected for the compressive strength according to ASTM D 1621. The densification is taken as the strain at the point of intersection between the tangents of the plateau region and the backward-extended densification strain.<sup>23,37</sup> The neat POPU foam and EFB30/POPU exhibited a smooth plateau region, but the latter showed a positive slope in the compressive stress–strain curve. A possible explanation is that the foam cell wall collapsed in the plateau region, and the increment in compressive stress at the densification stage corresponded to the matrix behavior after the opposing cell walls touched each other.<sup>37,38</sup> Therefore, densification could have a close relationship with the porosity of the foam. It is evident that EFB/POPU composite foams densified at lower strains with higher EFB fiber contents are in accordance with their porosity.

The compressive modulus and compressive strength at 10% strain for the neat POPU foam and EFB/POPU composite foams are recorded in Table I. The addition of EFB fiber led to a significant improvement in compressive modulus and strength of the EFB/POPU composite foam compared to neat POPU foam. The addition of 30 vol % of EFB could enhance up to five times the compressive modulus and nine times the compressive strength of the POPU foam. The improvement in the compressive property originated from the structure of EFB as a reinforcing fiber, good interfacial bonding, as well as parallel dispersion in the POPU matrix.

Table II presents the properties of biobased polyurethane from soybean oil and rapeseed oil versus palm oil. The visible advantages of the studied POPU are its mixing time and cream time compared to those of soybean oil and rapeseed oil-based polyurethane. Actually, the fast foaming reaction between polyol and isocyanate is the most challenging issue in the preparation of polyurethane and its composites. The cream time is normally less than 2 min, which is considered to be too fast to obtain good mixing and shaping processes for neat polyurethane and its composite products. In most of the polyurethane composites, additives and fillers are always mixed with a polyol prior, and isocyanate is consistently the last addition. The mixing time of isocyanate into the mixture was about 10–30 s, as reported in the literature.<sup>2,4,5,39</sup> However, the amount of isocyanate used is

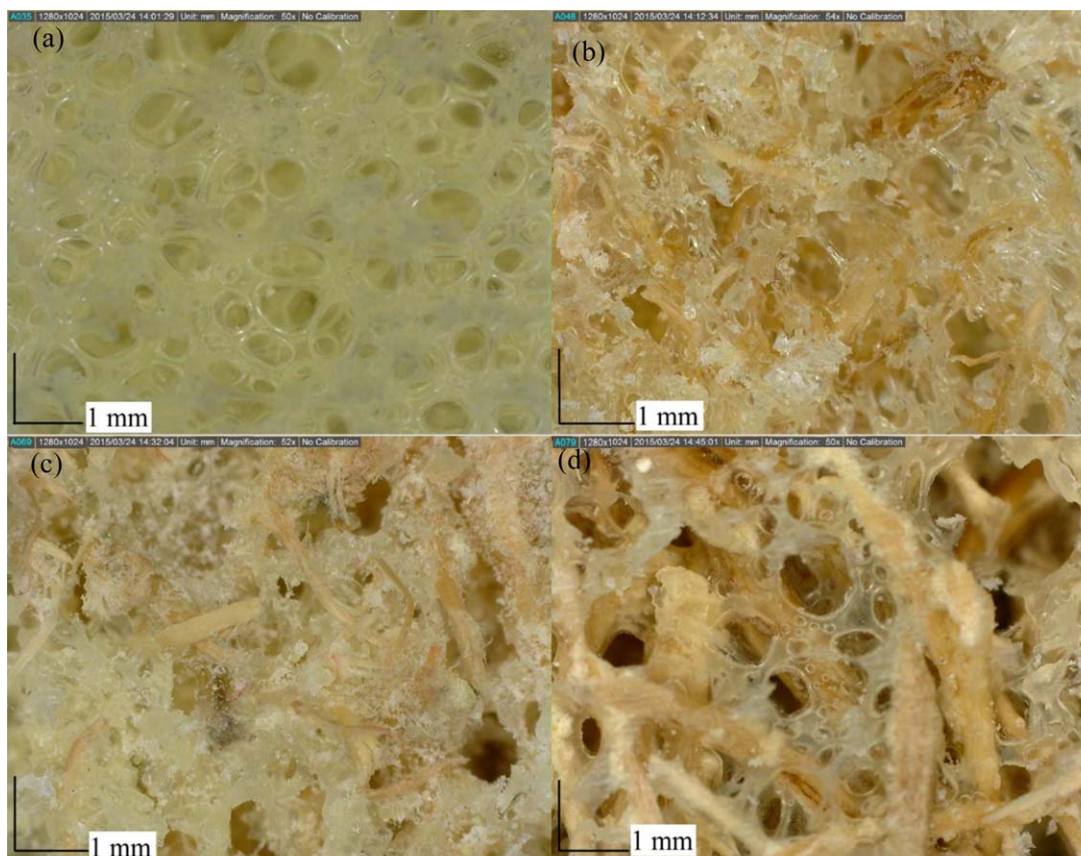


**Figure 3.** Cross sections of (a) neat POPU, (b) EFB15/POPU, (c) EFB20/POPU, and (d) EFB30/POPU at 50 $\times$  magnification. [Color figure can be viewed in the online issue, which is available at [wileyonlinelibrary.com](http://wileyonlinelibrary.com).]

usually more than the amount of polyol, with the ratio of 1 polyol to 1.05–1.50 isocyanates. Therefore, the filler's wetting by polyol and isocyanate and filler dispersion in the matrix after foam rising could have some limitation, especially for those nanofillers. This drawback will be more obvious for the samples and products with large dimensions. In this research, palm oil-based polyol and isocyanate were mixed for 3 min thanks to their long

cream time. The addition of EFB fibers afterward could provide good wetting and dispersing for the EFB fibers in the mixture. This practice is believed to be an effective factor in contributing the significant enhancement of EFB fibers in the POPU composite. In a comparison among palm oil-based versus soybean oil-based<sup>3,40</sup> and rapeseed oil-based PU composites,<sup>41,42</sup> the first displayed a greater performance in compressive modulus and strength than either of the latter. This enhancement originates from the higher filler loading of EFB in POPU, which could only be implemented when the cream time was long enough.

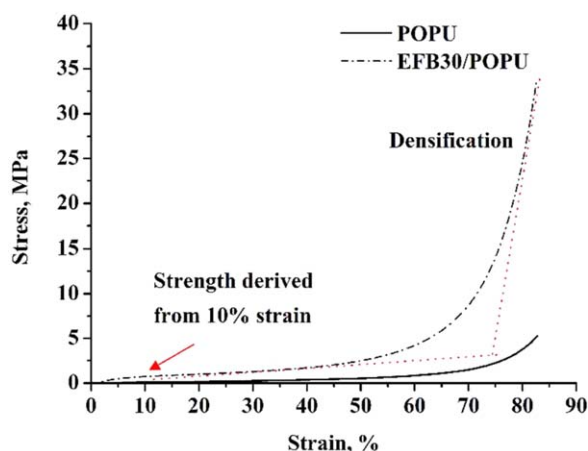


**Figure 4.** Typical stress–strain curves of neat POPU and EFB30/POPU composite foam. [Color figure can be viewed in the online issue, which is available at [wileyonlinelibrary.com](http://wileyonlinelibrary.com).]

**Flexural Properties of EFB/POPU Composite Foam.** It is clear that the EFB fiber exhibited a reinforcement effect on the flexural modulus and strength of the EFB/POPU composite foams, as reported in Table I. The flexural modulus of the composite foams improved as the EFB content increased from 15 to 30 vol %. The maximum increase was found, at approximately six times the flexural modulus and 10 times in flexural strength, when adding 30 vol % of EFB into the POPU foam. The enhancement in flexural properties of the composite foams originates from the high stiffness of the EFB fibers, which led the EFB/POPU composite foam to have a higher bending resistance. Similarly, the flexural properties of the epoxy syntactic foam reinforced by short glass fibers can also be obviously improved with respect to those of the unreinforced foam.<sup>43</sup> Furthermore, the obvious improvement in flexural toughness implies better stress transfer between the

**Table II.** Properties of Biobased Polyurethanes and Their Composites

Properties	Palm oil-based PU (present study)	Soybean oil-based PU	Rapeseed oil-based PU
With addition of petroleum-based polyol	—	—	30%, <sup>42</sup> 50% <sup>41</sup>
Hydroxyl number (mg KOH/g)	98	63, <sup>40</sup> 170 <sup>3</sup>	400 <sup>41</sup>
Isocyanate index	1.05	1.20 <sup>3,40</sup>	1.60, <sup>41</sup> 2.50 <sup>42</sup>
Mixing time of isocyanate (min)	3	0.33, <sup>40</sup> 1 <sup>3</sup>	0.25 <sup>41</sup>
Cream time (min)	7	1.50 <sup>40</sup>	—
Compressive modulus (MPa)	1.45	0.75 <sup>40</sup>	6.02 <sup>42</sup>
Compressive strength (kPa)	80	30, <sup>3</sup> 42 <sup>40</sup>	200, <sup>41</sup> 260 <sup>42</sup>
With fillers	30 vol % EFB	8 php paper fiber <sup>3</sup> 10 wt % wood flour <sup>40</sup>	1 wt % CNT <sup>41</sup> 6 wt % flax fiber <sup>42</sup>
Compressive modulus (MPa)	7.25	1.20 <sup>40</sup>	6.05 <sup>42</sup>
Compressive strength (kPa)	740	50, <sup>3</sup> 65 <sup>40</sup>	300 <sup>41,42</sup>

polyurethane matrix and the EFB fibers in the EFB/POPU composite foams via the good interfacial adhesion between the fiber and the foam matrix.

A crack developed at the bottom section of the composite foam under three-point bending, as shown in Figure 5, which experienced maximum deflection and maximum tension stress. The fracture was found to occur within the polyurethane matrix while the EFB remained unbroken, as observed in the SEM images in Figure 6. The presence of EFB fibers in the composite foam resulted in a serrated crack and hence improved the toughness of the EFB composite foam compared to the control POPU foam.

#### Mechanical Properties of UD Flax–Epoxy Composites

The tensile and flexural properties of the UD flax–epoxy composites as assessed by tensile testing and three-point bending (in both longitudinal and transverse directions), respectively, are given in Table III. With approximately 34% fiber volume fraction, the UD composite has a substantially high *E*-modulus of 20 GPa and a tensile strength of 194 MPa. A high strength in three-point bending in the longitudinal direction was also obtained, where the flexural modulus and flexural strength were approximately 19 GPa and 207 MPa, respectively. When UD composites are tested with the fibers in the transverse direction, the matrix and interface properties dominate the final composite properties. Hence, the interface quality of the

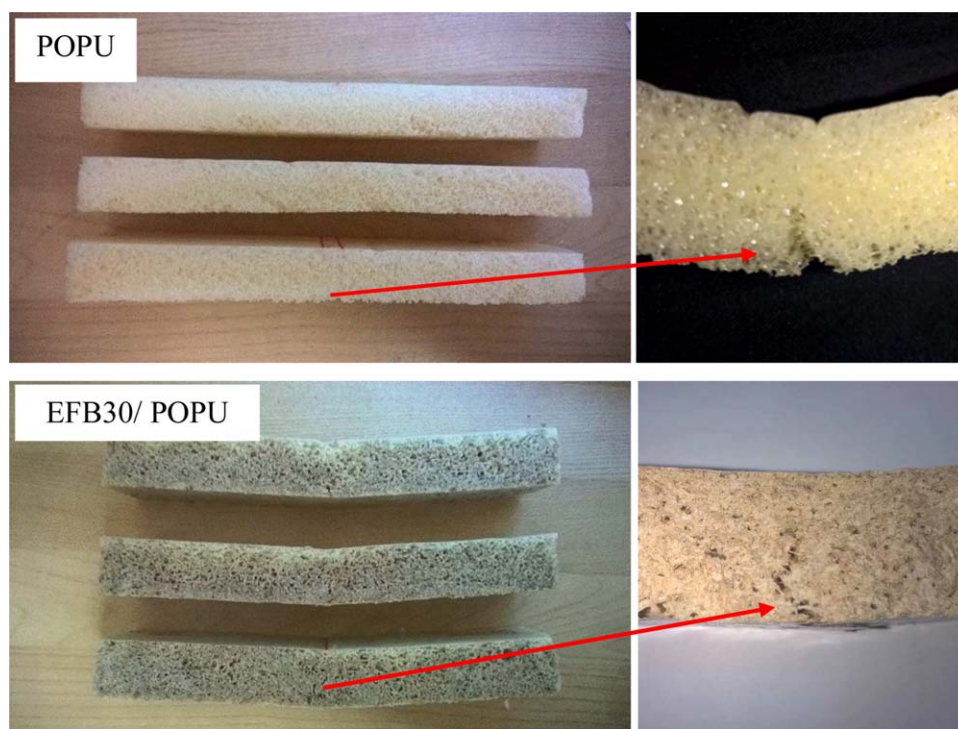


**Figure 5.** Tensile failure mode of neat POPU and EFB30/POPU composite foam. [Color figure can be viewed in the online issue, which is available at [wileyonlinelibrary.com](http://wileyonlinelibrary.com).]



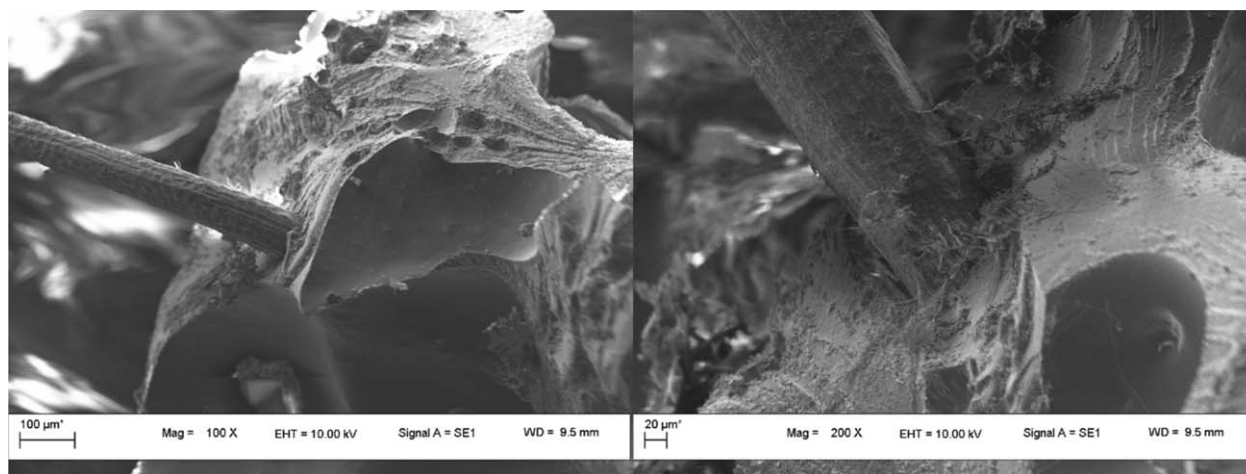


**Figure 6.** Flexural fractured surface of the EFB15/POPU composite foam at different magnifications.

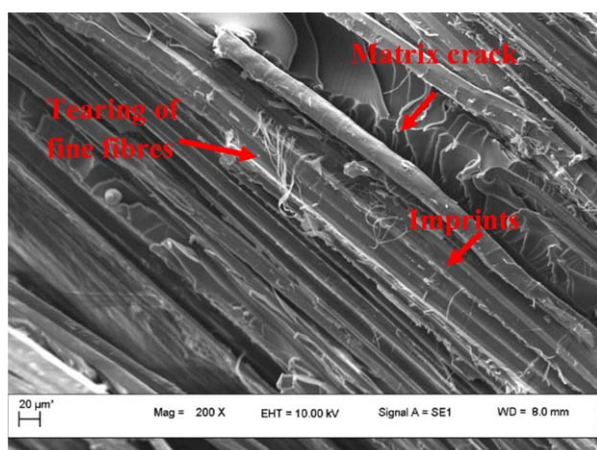


**Figure 7.** Fracture surface after transverse flexural test of flax-epoxy composite. [Color figure can be viewed in the online issue, which is available at [wileyonlinelibrary.com](http://wileyonlinelibrary.com).]

composite can be characterized by the transverse strength combined with the fracture morphology. SEM micrographs of the fracture surfaces of the transverse flexural sample can be seen in Figure 7. There is a clear imprint of the surface texture of the flax fiber remaining on the epoxy that indicates that failure occurs at the interface. Therefore, the transverse strength can be considered as the interfacial strength of the composite. The interfacial strength of the flax-epoxy composite is approximately 30 MPa, which is high compared to the reported values of interfacial strength for several natural fiber composite systems.<sup>44,45</sup> The mechanical properties of the UD flax-epoxy composite show that the composite is strong, stiff,

and suitable to be used as face sheets for lightweight sandwich constructions.

#### Flexural Properties and Failure Mode of Structural Sandwich between UD Flax-Epoxy Composites and Various Foam Cores

Typical flexural stress-strain curves of the sandwiches of UD flax-epoxy with 20% EFB composite foam (SW20), 30% EFB composite foam (SW30), and PET foam core (SW-PET) are shown in Figure 8. The stress-strain curves of SW20 and SW30 were obviously different from that of SW-PET. For the SW20 and SW30 sandwiches, the flexural stress increased gradually to reach the maximum stress at 4.27% and 3.19% deflection, respectively, decreasing gradually after that. However, the flexural stress of SW-PET exhibited a sharp drop after obtaining the maximum stress at 1.05% deflection. The deflections at break of SW20 and SW30 were higher than the deflection of the flax-epoxy composite face sheets (2.75%, as shown in Table III). This implied that the toughened EFB/POPU composite core had the potential to ameliorate the bending capability of face sheets in a sandwich structure. Besides, further bending strain causes shear stress to the core, due to different bending capabilities in the face sheets and core, which eventually produced a shear crack failure. In addition, SW30 exhibited higher flexural modulus, flexural strength, and flexural toughness than SW20. Therefore, 30 vol % could be considered as the optimum EFB fiber loading to obtain a high-strength composite foam core and sandwich. Based on the results of energy at break, it can be concluded that EFB has a pronounced toughening effect on the sandwich, and EFB/POPU composite foams have performance comparable to commercial PET core.

All the sandwiches exhibited core shear failure, and no indentation failure was observed, as shown in Figure 9. This implied that the

**Table III.** Mechanical Properties of Flax-Epoxy Composites Face Sheet

Test	Mechanical properties	Modulus (Gpa)	Strength (MPa)	Deflection at break (%)
Tensile	Longitudinal	20.06 ( $\pm 1.49$ )	193.79 ( $\pm 17.97$ )	0.83 ( $\pm 0.05$ )
Flexural	Longitudinal	19.03 ( $\pm 1.53$ )	207.17 ( $\pm 26.90$ )	2.90 ( $\pm 0.07$ )
	Transverse	2.81 ( $\pm 0.22$ )	30.59 ( $\pm 1.85$ )	1.30 ( $\pm 0.03$ )

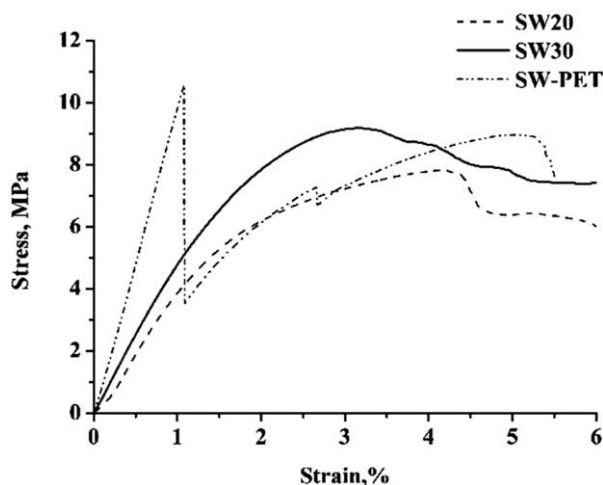


**Figure 8.** Typical three-point bending stress–strain curves of SW20, SW30, and SW-PET using EFB20/POPU, EFB30/POPU, and SW-PET using PET foam cores, respectively.

EFB/POPU composite foams are considered as high-compressive-strength cores, as is PET foam core. A similar failure was observed in a sandwich that was made up of glass fiber composite skins and modified phenolic core material, indicating that sandwiches comprising a high-compressive-strength core could prevent any localized failure in the core.<sup>24</sup> The failure mechanism of SW20 and SW30 showed that the crack occurred initially in the EFB/POPU composite foam around the loading nose and propagated to one

side of the sandwich's overhang. However, in SW-PET, the crack initially occurred at the interface of the top face sheet and the PET foam core right at the loading nose and further caused core shear failure in PET foam core and finally debonding at the interface of PET foam core and bottom face sheet until the overhang. Moreover, the toughening effect of the composite core in SW30 was evident from the lower shear crack angle of 35° compared to the value of 40° for the SW-PET foam core. The lower shear crack angle could be attributed to the bending capability of the EFB30/POPU composite core as a result of its flexural toughness.

Nowadays, research on plant oil-based polyurethanes and their composites has increased rapidly, but the study of their application as cores for structural sandwiches has been less reported. The composite foam cores for structural sandwiches in most of the studies, which are concerned about environmental issues, were petroleum-based polyurethane filled natural fiber, unfilled phenolic foam, or unfilled recycled PET foam. Nevertheless, apart from these environmentally friendly foam cores, the face sheet materials in structural sandwiches are still mainly used from synthesized fiber reinforced polymer composites. Table IV displays some reference sandwiches using foam cores from petroleum-based polyurethane filled coir fiber<sup>46</sup> or basalt fiber<sup>47</sup> attached to glass fiber–epoxy face sheets and a sandwich using commercial modified phenolic foam from plant products attached to glass fiber–phenol formaldehyde face sheets.<sup>24</sup> The SW30 sandwich having natural fiber reinforcement in both face sheets and core was found to have a better flexural strength than that of sandwiches using petroleum-based polyurethane

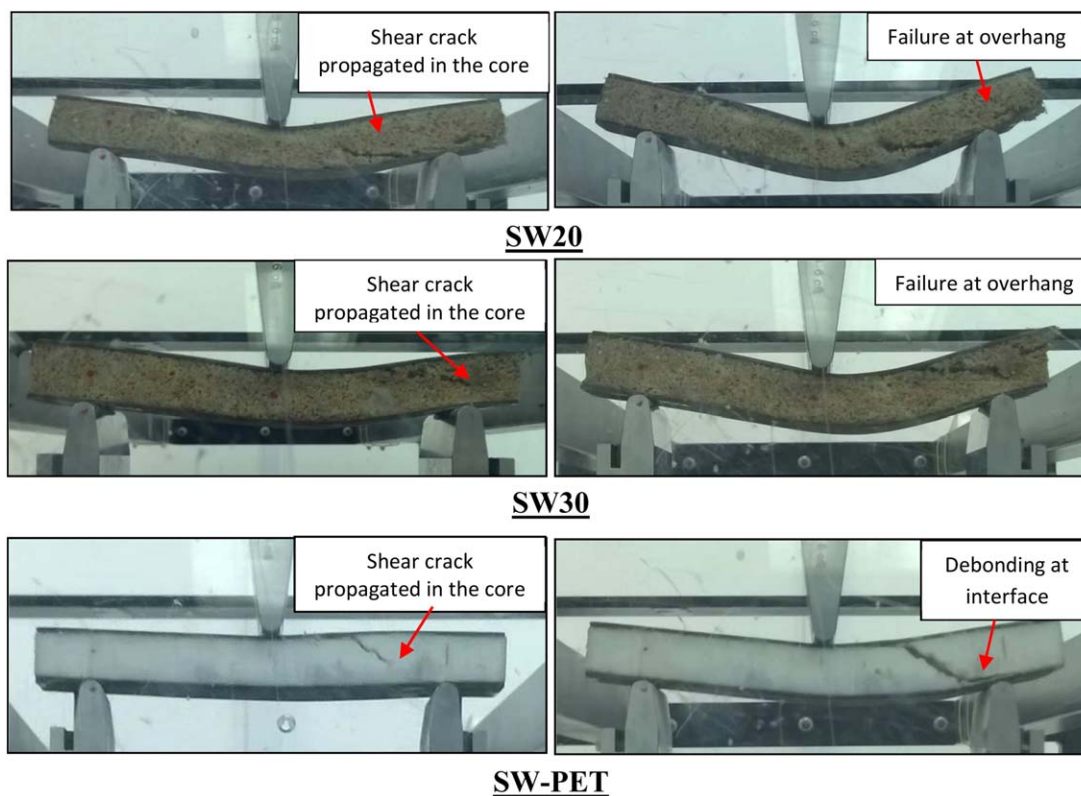


**Figure 9.** Failure mechanism of SW20, SW30, and SW-PET sandwich under three-point bending test. [Color figure can be viewed in the online issue, which is available at [wileyonlinelibrary.com](http://wileyonlinelibrary.com).]

**Table IV.** Structural Sandwich Using Petroleum-Based Polyurethane Composite and Commercial Phenolic Foam Core

Composite core	Palm oil-based PU filled 30 vol % EFB	Petroleum-based PU filled 20 wt % coir fiber <sup>46</sup>	Petroleum-based PU filled 20 wt % basalt fiber <sup>47</sup>	Commercial modified phenolic foam from plant products <sup>24</sup>
Composite face sheets	34 vol % UD flax-epoxy	67 wt % woven glass fiber mat/epoxy	50 vol % of bi-axial (0/90) E-glass fabric/epoxy	Biaxial (0/90) E-CR glass fabrics with a chopped strand mat/phenol formaldehyde
Density of sandwich (g cm <sup>-3</sup> )	0.44	0.38	0.15	—
Flexural load (kN)	1.097	0.72–0.85	—	13.18–14.20
Flexural modulus (MPa)	507.55	520–580	≈8	—
Flexural strength (MPa)	9.16	0.24–0.29	≈1.28	—
Shear crack angle	35°	—	—	≈55°

composites and to have a lower shear crack angle than that of the reference sandwich using a commercial phenolic foam from plant products. Hence, the SW30 sandwich, with its good mechanical performance, more green constituents, and low cost, could be proposed for civil applications.

#### Evaluation of Maximum Face Yield Load of Face Sheet and Shear Strength Carried by Core during Bending of Structural Sandwich

The calculated flexural strength and the maximum load yielded by the UD flax-epoxy face sheet and shear strength carried by a core of the sandwiches are shown in Table V. The calculated flexural strengths of the face sheets in the sandwiches were only about 11–15% of the bending strength of the UD flax-epoxy composite (207.17 MPa, as listed in Table III). This clearly indicates that no tensile crack failure mode occurred at the bottom face sheet. The calculated maximum loads for face yield were found to be higher than those exerted on the sandwiches (Table V). This result indicates that there was no failure of microbuckling at the top face sheet or face yield at the bottom face sheet in all sandwiches.<sup>48</sup> Therefore, a core shear failure was the only failure to have occurred in these sandwiches. The calculated shear strengths obtained from EFB/POPU composite cores and

commercial PET foam core were comparable. This toughening effect of the properties of the EFB/POPU composite core suggests that this composite core has the potential for economic, green, and high-strength structural sandwich applications.

#### CONCLUSIONS

EFB fiber POPU foam. The flexural and compressive strength and modulus of POPU foam were enhanced significantly with the addition of 15–30 vol % EFB to the EFB/POPU composites. When applied as a core in a structural sandwich, the sample SW30 exhibited a higher flexural energy at break and a lower shear crack angle than the SW-PET sandwich. Furthermore, the high-toughness EFB/POPU composite core prevented debonding between the face sheet and the core, which occurred obviously in the SW-PET sandwich. These advanced mechanical properties imply that EFB/POPU biobased composite foams are economic, green, and high-strength cores for structural sandwiches. Based on the evaluation of the endured strength of the face sheet and core in the sandwich structure, a thinner face sheet could be implemented. Moreover, the addition of palm oil biomass such as palm kernel shell into the EFB/POPU composite foam could be carried out and could be expected to achieve

**Table V.** Flexural Properties of Structural Sandwiches and Calculated Strength of Face Sheet and Cores

Properties	SW20	SW30	SW-PET
Load (kN)	0.680 (±0.04)	1.097 (±0.12)	1.467 (±0.05)
Flexural modulus (MPa)	316.7 (±68.9)	507.6 (±82.5)	838.8 (±109.7)
Flexural strength (MPa)	8.15 (±0.65)	9.16 (±0.46)	11.16 (±0.50)
Deflection at flexural strength (%)	4.27 ± (0.01)	3.19 ± (0.01)	1.05 (±0.01)
Energy at break (J)	3.32 (±0.71)	3.56 (±0.22)	1.61 (±0.74)
Shear crack angle	38°	35°	40°
Calculated strength of face Sheets and core in structural sandwich			
Flexural strength for face sheet (MPa)	23.46 (±4.14)	24.88 (±2.44)	33.02 (±1.21)
Max. load for face yield (kN)	1.03 (±0.13)	1.29 (±0.19)	1.94 (±0.07)
Core shear strength (MPa)	0.47 (±0.06)	0.52 (±0.08)	0.73 (±0.03)

SW20 has EFB20/POPU foam core, SW30 has a EFB30/POPU foam core, and SW-PET has a PET foam core.

significant compressive strength and modulus for the composite foam and its derived sandwich.

## ACKNOWLEDGMENTS

This research is supported by the Ministry of Higher Education Malaysia through the Fundamental Research Grant Scheme (FRGS) 9003-00326. We would also like to acknowledge PolyGreen Chemicals (Malaysia) Sdn. Bhd. for providing palm oil-based polyol.

## REFERENCES

1. Ionescu, M. In *Chemistry and Technology of Polyols for Polyurethanes*; Ionescu, M., Ed.; Smithers Rapra Technology, Shrewsbury, UK **2005**; pp 13–30.
2. Veronese, B.; Menger, R. K.; Forte, M. M. D. C.; Petzhold, C. L. *J. Appl. Polym. Sci.* **2010**, *120*, 530.
3. Banik, I.; Sain, M. M. *J. Appl. Polym. Sci.* **2009**, *112*, 1974.
4. Kuranska, M.; Prociak, A. *Compos. Sci. Technol.* **2012**, *72*, 299.
5. Kuranska, M.; Prociak, A.; Mikelis, K.; Ugis, C. *Compos. Sci. Technol.* **2013**, *75*, 70.
6. Zhang, L.; Zhang, M.; Hu, L.; Zhou, Y. J. *Ind. Crop. Prod.* **2014**, *52*, 380.
7. Zhu, M.; Bandyopadhyay-Ghosh, S.; Khazabi, M.; Cai, H.; Correa, C.; Sain, M. *J. Appl. Polym. Sci.* **2011**, *124*, 4702.
8. Abdul Khalil, H. P. S.; Poh, B. T.; Issam, A. M.; Jawaid, M.; Ridzuan, R. *J. Reinf. Plast. Compos.* **2010**, *29*, 1117.
9. Dungani, R.; Jawaid, M.; Khalil, H. P. S. A.; Aprilia, S. *Bio-Resources* **2013**, *8*, 3136.
10. Wan Aizuddin, W. R.; Azhari, S. B.; Ahmad, T. T.; Alawi, S.; Nazli Naim, M.; Mohd Ali, H.; Shirai, Y. *BioResources* **2012**, *7*, 4786.
11. Kim, S.; Kim, H. C. *J. Renew. Energy* **2013**, *54*, 150.
12. Khalil, H. P. S. A.; Alwani, M. S.; Omar, A. K. M. *BioResources* **2006**, *1*, 220.
13. Rozman, H. D.; Ahmadhilmil, K. R.; Abubakar, A. *Polym. Test.* **2004**, *23*, 559.
14. Kabir, M. M.; Wang, H.; Lau, K. T.; Cardona, F. *Compos. Part B Eng.* **2012**, *43*, 2883.
15. Zhu, J.; Zhu, H.; Njuguna, J.; Abhyankar, H. *Materials (Basel)* **2013**, *6*, 5171.
16. Badri, K. H.; Amin, K. A. M.; Othman, Z.; Manaf, H. A.; Khalid, N. K. *Polym. Int.* **2006**, *55*, 190.
17. Cheng, T. S.; Nurul Ain, N.; Lan, D. N. U.; Teh, P. L. J. *Malaysian J. Anal. Sci.* **2014**, *18*, 651.
18. Doddamani, M. R.; Kulkarni, S. M. In *Finite Element Analysis: Applications in Mechanical Engineering*; Farzad, E., Ed.; InTech Open Access Publisher, Croatia **2012**.
19. Wambua, P.; Ivens, J.; Verpoest, I. *Compos. Sci. Technol.* **2003**, *63*, 1259.
20. Kairyte, A.; Vėjelis, S. *Ind. Crops Prod.* **2015**, *66*, 210.
21. Hu, X.; Wouterson, E. M.; Liu, M. In *Handbook of Manufacturing Engineering and Technology*; Nee, A. Y. C., Ed.; Springer-Verlag: London, **2015**; p 125.
22. Xanthos, M.; Dhavalikar, R.; Tan, V.; Dey, S. K.; Yilmazer, U. *J. Reinf. Plast. Compos.* **2001**, *20*, 786.
23. Celzard, A.; Zhao, W.; Pizzi, A.; Fierro, V. *Mater. Sci. Eng. A* **2010**, *527*, 4438.
24. Manalo, A. C. J. *Compos. Struct.* **2013**, *99*, 339.
25. Daniel, I. M.; Gdoutos, E. E. In *Major Accomplishments in Composite Materials and Sandwich Structures*; Daniel, I. M., Gdoutos, E. E., Rajapakse, Y. D. S., Eds.; Springer Netherlands: Dordrecht, **2010**; p 197.
26. McCormack, T. M.; Miller, R.; Kesler, O.; Gibson, L. J. *Int. J. Solid Struct.* **2001**, *38*, 4901.
27. Konsta-Gdoutos, M. S.; Gdoutos, E. E. *Appl. Compos. Mater.* **2005**, *12*, 165.
28. Li, X.; Tabil, L. G.; Panigrahi, S. *J. Polym. Environ.* **2007**, *15*, 25.
29. Bakare, I. O.; Okieimen, F. E.; Pavithran, C.; Abdul Khalil, H. P. S.; Brahmakumar, M. *Mater. Des.* **2010**, *31*, 4274.
30. El-Meligy, M. G.; El-Zawawy, W. K.; Ibrahim, M. M. *J. Polym. Adv. Technol.* **2004**, *15*, 738.
31. Wong, C. S. *Mater. Sci. Appl.* **2012**, *03*, 78.
32. El-Shekeil, Y. A.; Sapuan, S. M.; Khalina, A.; Zainudin, E. S.; Al-Shuja'a, O. M. *EXPRESS Polym. Lett.* **2012**, *6*, 1032.
33. Silva, M. C.; Takahashi, J. A.; Chaussy, D.; Belgacem, M. N.; Silva, G. G. *J. Appl. Polym. Sci.* **2010**, *117*, 3665.
34. Wang, X.; Ren, H. *Appl. Surf. Sci.* **2008**, *254*, 7029.
35. Tan, C.; Ahmad, I.; Heng, M. *Mater. Des.* **2011**, *32*, 4493.
36. Ribeiro, V.; Mosiewicki, M. A.; Irene, M.; Coelho, M.; Stefani, P. M.; Marcovich, N. E. *J. Polym. Test.* **2013**, *32*, 438.
37. Chen, L.; Hoo, M. S. *J. Mater. Sci.* **2013**, *48*, 6786.
38. Dariushi, S.; Sadighi, M. *Appl. Compos. Mater.* **2012**, *20*, 839.
39. Zhou, X.; Sain, M. M.; Oksman, K. *Compos. Part A: Appl. Sci. Manuf.* **2015**, *83*, 56.
40. Chang, L.-C.; Sain, M.; Kortschot, M. J. *Cell. Plast.* **2015**, *51*, 103.
41. Cabulis, U.; Sevastyanova, I.; Andersons, J.; Beverte, I. *Polimery* **2014**, *59*, 207.
42. Kuranska, M.; Prociak, A. *Tech. Trans. Chem.* **2015**, *112*, 47.
43. Wang, L.; Zhang, J.; Yang, X.; Zhang, C.; Gong, W.; Yu, J. *Mater. Des.* **2014**, *55*, 929.
44. Hossain, R.; Islam, A.; Vuure, A.; Van; Verpoest, I. *ARPN J. Eng. Appl. Sci.* **2013**, *8*, 513.
45. Tran, L. Q. N.; Fuentes, C. A.; Dupont-Gillain, C.; Vuure, A. W.; Van; Verpoest, I. *Compos. Sci. Technol.* **2013**, *80*, 23.
46. Azmi, M. A.; Abdullah, H. Z.; Idris, M. I. *IOP Conf. Ser. Mater. Sci. Eng.* **2013**, *50*, 012067.
47. Lopresto, V.; Leone, C.; Caprino, G.; De Iorio, I. *Procedia Eng.* **2011**, *10*, 2058.
48. Steeves, C. A.; Fleck, N. A. *Int. J. Mech. Sci.* **2004**, *46*, 585.